INSTITUTE OF PHYSICS PUBLISHING SEMICONDUCTOR SCIENCE AND TECHNOLOGY

Semicond. Sci. Technol. **21** (2006) 906–911 doi:10.1088/0268-1242/21/7/014

Atomistic calculation of elastic moduli in strained silicon

R Zhu[1], E Pan[1], P W Chung[2], X Cai[3], K M Liew[4] and A Buldum[5]

[1] Department of Civil Engineering, University of Akron, Akron, OH 44325, USA
[2] US Army Research Laboratory, Aberdeen Proving Ground, MD 21005, USA
[3] School of Mechanical & Aerospace Engineering, Nanyang Technology University, Singapore
[4] Department of Building and Construction, City University of Hong Kong, Tat Chee Avenue, Kowloon, Hong Kong, People's Republic of China
[5] Department of Physics, The University of Akron, Akron, OH 44325, USA

E-mail: pan2@uakron.edu

Received 23 January 2006, in final form 24 January 2006
Published 5 June 2006
Online at stacks.iop.org/SST/21/906

Abstract

Strained silicon is becoming a new technology in silicon industry where the novel strain-induced features are utilized. In this paper we present a molecular dynamic prediction for the elastic stiffnesses C_{11}, C_{12} and C_{44} in strained silicon as functions of the volumetric strain level. Our approach combines basic continuum mechanics with the classical molecular dynamic approach, supplemented with the Stillinger–Weber potential. Using our approach, the bulk modulus, effective elastic stiffnesses C_{11}, C_{12} and C_{44} of the strained silicon, including also the effective Young's modulus and Poisson's ratio, are all calculated and presented in terms of figures and formulae. In general, our simulation indicates that the bulk moduli, C_{11} and C_{12}, increase with increasing volumetric strain whilst C_{44} is almost independent of the volumetric strain. The difference between strained moduli and those at zero strain can be very large, and therefore use of standard free-strained moduli should be cautious.

(Some figures in this article are in colour only in the electronic version)

1. Introduction

Strained quantum nanostructures have led to intensive studies in recent years due to their improved electronic and optical properties arising from quantum confinements [1]. The importance of strain in semiconductors has been widely recognized, and its influence on the electronic and optical properties was also carried out. Specifically, the distortion of the crystalline structure changes the properties of the charge carriers in silicon, allowing the carriers to move more quickly in response to an applied voltage. These charge carriers, electrons (negative charge carriers) and holes (positive charge carriers), are reported to have a higher mobility when silicon is strained [2–5]. In 2003, IBM and AMD reported the most exciting news on the application of strained silicon where they successfully integrated the strained silicon into their design [6]. This new advance improves transistor performance by 10–25% whilst the corresponding increase in manufacturing costs is only about 2%. While the performance of strained silicon in terms of its electronic and optical properties is an active topic, the corresponding mechanical behaviour has rarely been studied. Yet, understanding the mechanical properties of strained silicon is very important with regard to its long-term performance and structure reliability.

Silicon can be strained in compression (i.e., the atoms are being squeezed together) or in tension (i.e., the atoms are being stretched apart). The most established and proven method of straining silicon involves the deposition of a silicon–germanium (SiGe) film on the top of a traditional silicon wafer, which then acts as an atomic template for deposition of a subsequent thin film of silicon. The thin film of silicon conforms to the atomic spacing of the underlying SiGe layer and assumes a state of biaxial tension (i.e., silicon is stretched in two orthogonal directions, as shown in figure 1).

While variation of the elastic moduli was studied previously when silicon was under pressure [7, 8], no literature

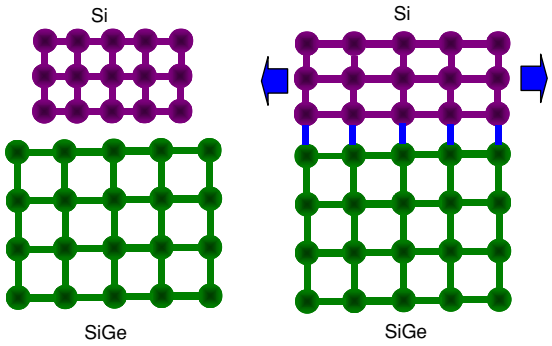

Figure 1. Stretched silicon for silicon over a silicon–germanium substrate.

is available on the stress and strain behaviour when silicon is under strain. Furthermore, due to the technical difficulty, it is hard to observe experimentally the elastic properties as functions of the applied strain.

In this paper, therefore, we present a molecular dynamic simulation for the elastic stiffnesses in strained silicon as functions of the volumetric strain level (corresponding to the misfit strain due to the lattice constant difference between silicon and its substrate). Our method combines the basic continuum mechanics with the classical molecular dynamic simulation, supplemented with the interatomic Stillinger–Weber potential [9]. The S–W potential has gained popularity due to its ability to describe fairly well the diamond structure (e.g., [10–12]). In order to use our method for the estimation of the three independent elastic stiffnesses C_{11}, C_{12} and C_{44} in strained silicon, we apply three independent distortions as described by Mehl [13, 14] and utilized more recently by Ellaway and Faux [15] for InAs. The elastic stiffnesses, effective Young's modulus and Poisson's ratio are all calculated and presented in terms of figures and formulae. In general, our simulation indicates that the bulk moduli, C_{11} and C_{12}, increase with increasing volumetric strain whilst C_{44} is almost independent of volumetric strain. The difference between strained moduli and those at zero strain can be very large, and therefore use of standard free-strained moduli in the strained silicon could result in the wrong mechanical response in silicon. Using strained moduli could also predict different electronic and optical properties in the strained silicon.

2. Elastic stiffness calculation

The IV and III–V semiconductors, in their cubic structure, have three independent elastic stiffnesses C_{11}, C_{12} and C_{44}. It was shown that when the crystal is strained, its elastic stiffnesses can be substantially changed (e.g., [15]). To predict the accurate change of the material stiffness due to straining, the so-called direct and traditional method can be followed where a tension/compression is applied to the material. The system energy is then calculated, which is utilized finally to predict the stress–strain relationship [14–16].

For a cubic crystal, the elastic moduli can be divided into two classes: the bulk modulus $B = (C_{11} + 2C_{12})/3$ and two 'shear' moduli C_{11}–C_{12} and C_{44}. In the actual calculation, a small incremental distortion, which is usually less than 1%, is applied to the crystal with the latter being already subjected to a uniform volumetric strain (i.e., [15]).

Let us assume that the original cubic lengths and the distortions in the (x, y, z)-directions are $(\Delta x, \Delta y, \Delta z)$ and $(\varepsilon_x, \varepsilon_y, \varepsilon_z)$, respectively. After deformation, the new volume becomes

$$\begin{aligned} V &= \Delta x(1+\varepsilon_x)\Delta y(1+\varepsilon_y)\Delta z(1+\varepsilon_z) \\ &= \Delta x\Delta y\Delta z(1+\varepsilon_x+\varepsilon_y+\varepsilon_z+\varepsilon_x\varepsilon_y \\ &\quad +\varepsilon_y\varepsilon_z+\varepsilon_z\varepsilon_x+\varepsilon_x\varepsilon_y\varepsilon_z). \end{aligned} \tag{1}$$

It is clear that for small deformation, we have the well-known volumetric strain

$$e = \frac{V - V_0}{V_0} = \varepsilon_x + \varepsilon_y + \varepsilon_z, \tag{2}$$

where $V_0 = \Delta x\Delta y\Delta z$ is the original volume of the unit cell.

The constitutive relation for the cubic material is

$$\begin{bmatrix} \sigma_{xx} \\ \sigma_{yy} \\ \sigma_{zz} \\ \tau_{yz} \\ \tau_{zx} \\ \tau_{xy} \end{bmatrix} = \begin{bmatrix} C_{11} & C_{12} & C_{12} & 0 & 0 & 0 \\ C_{12} & C_{11} & C_{12} & 0 & 0 & 0 \\ C_{12} & C_{12} & C_{11} & 0 & 0 & 0 \\ 0 & 0 & 0 & C_{44} & 0 & 0 \\ 0 & 0 & 0 & 0 & C_{44} & 0 \\ 0 & 0 & 0 & 0 & 0 & C_{44} \end{bmatrix} \begin{bmatrix} \varepsilon_{xx} \\ \varepsilon_{yy} \\ \varepsilon_{zz} \\ \gamma_{yz} \\ \gamma_{zx} \\ \gamma_{xy} \end{bmatrix} \tag{3}$$

with the corresponding strain energy per unit volume being

$$U = \tfrac{1}{2}(\sigma_{xx}\varepsilon_{xx} + \sigma_{yy}\varepsilon_{yy} + \sigma_{zz}\varepsilon_{zz} + \tau_{yz}\gamma_{yz} + \tau_{zx}\gamma_{zx} + \tau_{xy}\gamma_{xy}). \tag{4}$$

In the following, we briefly list the relevant formulae needed to obtain the elastic coefficients for the cubic crystal.

2.1. Bulk modulus B

The bulk modulus, B, is related to the curvature of the energy function $E(V)$ as [17]

$$B(V) = -VP'(V) = VE''(V), \tag{5}$$

where V is again the deformed volume of unit cell as mentioned before, $E(V)$ is the corresponding energy per unit cell, $E''(V)$ is the second derivative of $E(V)$ with respect to the volume and $P(V) = -E'(V)$ is the pressure. Since the calculation only provides a set of energies $E(V_i)$ for a limited number of volumes V_i, the second derivative $E''(V)$ must be approximated [14]. Birch [17] proposed the following equation to calculate $E(V)$ by fitting the curve:

$$\begin{aligned} E(V) &= E_0 + \frac{9}{8}B_0V_0\left[\left(\frac{V_0}{V}\right)^{2/3} - 1\right]^2 + \frac{9}{16}B_0V_0(B_0' - 4) \\ &\quad \times \left[\left(\frac{V_0}{V}\right)^{2/3} - 1\right]^3 + \sum_{n=4}^{N}\gamma_n\left[\left(\frac{V_0}{V}\right)^{2/3} - 1\right]^n, \end{aligned} \tag{6}$$

where E_0, V_0, B_0 and B_0' are, respectively, the equilibrium energy, volume, bulk modulus and pressure derivative of the bulk modulus, whilst N is the fitting order. We remark that equation (6) is a special case of the following general expression:

$$E(V) = \sum_{n=0}^{N} a_n V^{-2n/3}, \tag{7}$$

where a_n are the fitting parameters.

Therefore, the bulk modulus can be predicted on the basis of equation (7). In our atomistic MD simulation, the distortion used for calculating the bulk modulus consists of a uniform

compression (or expansion) of magnitude δ in each of the x-, y- and z-directions as in a conventional pressure experiment.

2.2. Modulus C_{11}–C_{12}

The 'shear' modulus C_{11}–C_{12} is evaluated by applying an orthorhombic volume-conserving (up to the first order of δ) strain which can be represented in the strain tensor form as

$$\begin{pmatrix} \delta & 0 & 0 \\ 0 & -\delta & 0 \\ 0 & 0 & \frac{\delta^2}{1-\delta^2} \end{pmatrix}. \tag{8}$$

Making use of the stress and strain relation, we found that the nonzero stresses are

$$\begin{aligned} \sigma_{xx} &= (C_{11} - C_{12})\delta + C_{12}\frac{\delta^2}{1-\delta^2} \\ \sigma_{yy} &= (C_{12} - C_{11})\delta + C_{12}\frac{\delta^2}{1-\delta^2} \\ \sigma_{zz} &= C_{11}\frac{\delta^2}{1-\delta^2}. \end{aligned} \tag{9}$$

From the strains and stresses, the corresponding system energy as a function of δ can be found as

$$E(\delta) = E(0) + (C_{11} - C_{12})V\delta^2 + 0(\delta^4) + \cdots, \tag{10}$$

where the terms of order δ^4 or higher can be safely neglected. Therefore, the energy $E(\delta)$ can be expressed as a function of δ^2 and a linear fitting of the curve yields C_{11}–C_{12}.

2.3. Elastic stiffness C_{44}

Finally, the elastic stiffness C_{44} is evaluated by a monoclinic volume-conserving (again, up to the first order of δ) strain, expressed in terms of the strain tensor as

$$\begin{pmatrix} 0 & \frac{1}{2}\delta & 0 \\ \frac{1}{2}\delta & 0 & 0 \\ 0 & 0 & \frac{\delta^2}{(4-\delta^2)} \end{pmatrix}. \tag{11}$$

Again, substituting this strain tensor into the stress and strain relation gives the only nonzero stress component (shear stress) as $\tau_{xy} = C_{44}\delta$, and the corresponding total energy

$$E(\delta) = E(0) + \tfrac{1}{2}C_{44}V\delta^2 + 0(\delta^4) + \cdots. \tag{12}$$

Similarly, the energy $E(\delta)$ can be expressed as a function of δ^2 and a linear fitting of the curve yields C_{44}.

3. Molecular dynamics programming

In order to use the molecular dynamics (MD) to simulate and predict the energy for a given distortion, we have to define the rules which govern the interaction among the atoms in the system. In the classical MD simulation, these rules are often expressed in terms of the potential function. The potential function $U(\mathbf{r}_i)$ describes how the potential energy of a system of N atoms depends on the coordinates of the atoms. In the past, various empirical potentials have been proposed to describe the different phases of silicon [9, 18–20] and results have been tested and compared [21–23]. Among these, the Stillinger and Weber (SW) potential [9] has gained popularity due to its ability to describe fairly well the diamond structure [10–12, 16, 21]. The main advantage of this potential

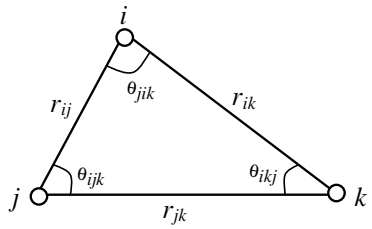

Figure 2. Geometric illustration of a triplet of atoms used in the definition of the three-body potential.

is its simplicity and fairly realistic description of the crystal. The potential consists of a two-body term and a three-body term as angular interaction:

$$\begin{aligned} U &= \sum_{i<j} v_2(r_{ij}) + \sum_{i<j<k} v_3(\mathbf{r}_i, \mathbf{r}_i, \mathbf{r}_k) \\ v_2(r_{ij}) &= \varepsilon f_2(r_{ij}/\sigma), \\ v_3(\mathbf{r}_i, \mathbf{r}_j, \mathbf{r}_k) &= \varepsilon f_3(\mathbf{r}_i/\sigma, \mathbf{r}_j/\sigma, \mathbf{r}_k/\sigma) \end{aligned} \tag{13}$$

where v_2 is the pair potential and v_3 is the three-body part. The functions f_2 and f_3 are defined as

$$f_2(r) = \begin{cases} A(Br^{-p} - r^{-q})\exp[(r-a)^{-1}], & r < a \\ 0, & r \geqslant a \end{cases}$$

$$f_3(\mathbf{r}_i, \mathbf{r}_j, \mathbf{r}_k) = \begin{cases} h(r_{ij}, r_{ik}, \theta_{jik}) + h(r_{ji}, r_{jk}, \theta_{ijk}) \\ \quad + h(r_{ki}, r_{kj}, \theta_{ikj}), & r < a, \\ 0, & r \geqslant a \end{cases} \tag{14}$$

where r is the distance between any two atoms; r_{ij} is the distance between the two atoms with indices i and j; $\mathbf{r}_i$, $\mathbf{r}_j$, $\mathbf{r}_k$ are the positions of atoms i, j and k, respectively; and θ_{jik} is the bond angle between vectors $\mathbf{r}_{ij}$ and $\mathbf{r}_{ik}$ (figure 2). Finally, the function h is the three-body potential part given as

$$\begin{aligned} h(r_{ij}, r_{ik}, \theta_{jik}) &= \lambda \exp[\gamma(r_{ij} - a)^{-1} + \gamma(r_{ik} - a)^{-1}] \\ &\quad \times \left(\cos\theta_{jik} + \tfrac{1}{3}\right)^2. \end{aligned} \tag{15}$$

The parameters A, B, p, q, a, λ, γ, ε and σ are all positive and are determined by ensuring that the diamond structure is the most stable periodic arrangement of particles at low pressure. For silicon, these parameters were given by Stillinger and Weber [9]: $a = 1.8$, $\gamma = 1.20$, $p = 4$, $q = 0$, $A = 7.049\,556\,277$, $B = 0.602\,224\,5584$, $\lambda = 21.0$, $\varepsilon = 50$ kcal mol^{-1} $= 3.4723 \times 10^{-19}$ J, $\sigma = 2.0951$ Å.

In our MD program, we first prepare a sample: we select a model system (a cubic structure) consisting of $N = 8 \times 3^3 = 216$ atoms under the periodic boundary condition, and we solve Newton's equation of motion for this system until the properties of the system no longer change with time (i.e., the equilibrium state). We then predict the system energy by applying a distortion to the system and solving Newton's equation of motion. In the simulation process, time step is one of the key factors. If the time step is too large, accurate results cannot be obtained; on the other hand, if it is too small, the MD simulation becomes too expensive to be carried out. In our program, we assume that the biggest one-step movement of any atom is about 0.05% of the equilibrium distance among the atoms, which is used to derive the time step in the paper. A number of examples have been run and results show that this criterion is accurate with reasonable CPU time. Furthermore, we have also run the MD program for a large size system

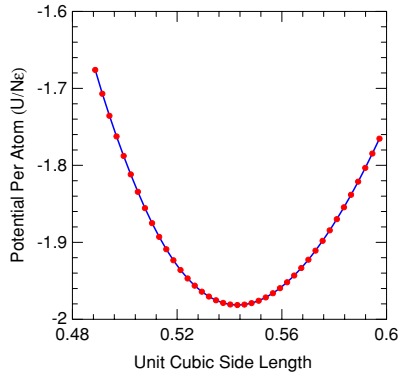

Figure 3. Lattice energy (per atom) versus single silicon cubic lattice length.

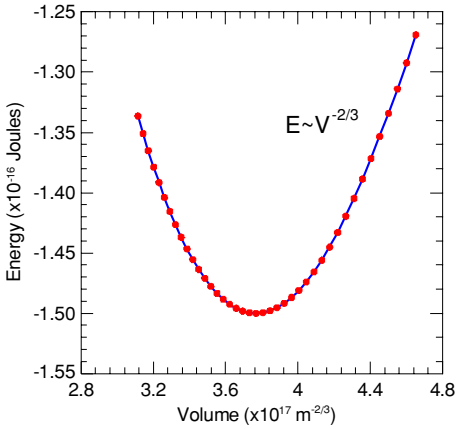

Figure 4. Lattice energy E (216 atom system) versus system volume ($V^{-2/3}$).

($N = 8 \times 5^3$) and found that the MD result for this system was close to that for the small size system ($N = 8 \times 3^3$); however, the large system required much more CPU time than the small system.

4. Results and discussion

4.1. Potential and cubic volume

In applying the MD to the bulk modulus calculation, we compress the model system uniformly in the x-, y-, and z-directions step by step and determine the system energy at the same time. Figure 3 shows the corresponding binding energy per atom $U/N\varepsilon$ (in reduced unit) versus unit cubic lattice length. It is clear that if the volumetric strain is zero (corresponding to free-strain lattice constant 0.5431 nm), the system in the equilibrium state has the lowest potential. Figure 4 shows the MD-simulated system potential versus system volume ($V^{-2/3}$). We further remark that the system potential as a function of the volume ($V^{-2/3}$) can also be accurately represented by a cubic function using equation (6) or (7), with the following coefficients obtained via curve fitting:

$$a_0 = 5.99 \times 10^{-16}, \qquad a_1 = -4.66 \times 10^{-33},$$
$$a_2 = 8.89 \times 10^{-51}, \qquad a_3 = -4.79 \times 10^{-69}. \tag{16}$$

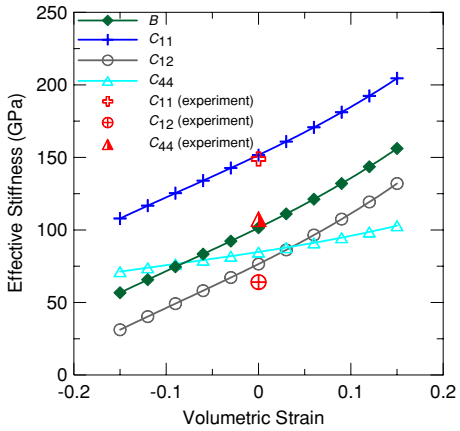

Figure 5. Bulk modulus B and other elastic moduli C_{11}, C_{12} and C_{44} as functions of the applied volumetric strain in the strained silicon.

4.2. C_{11}, C_{12} and C_{44}

Now, making use of equation (5) with the coefficients in equation (16), the relation between the bulk modulus $B = (C_{11} + 2C_{12})/3$ and volumetric strain of silicon can be obtained. Similarly, applying the deformation in equation (8) to the MD program, the atomistic simulation yields the energy (10), from which the 'shear' modulus C_{11}–C_{12} can be determined as a function of the applied strain δ. The results for the bulk modulus (C_{11} + 2C_{12})/3 and the 'shear' modulus C_{11}–C_{12} enable us to determine the elastic coefficients C_{11} and C_{12}. Finally, the pure shear coefficient C_{44} is directly obtained from (11) using the MD-simulated energy (12). The results for the stiffness coefficients as functions of the applied strain are presented in figure 5.

It is observed from figure 5 that at zero volumetric strain, our atomistic simulation predicts that $C_{11} = 151.6$ GPa and $C_{12} = 76.5$ GPa and $C_{44} = 84.8$ GPa. These coefficients are in close agreement with the experimental values of 166.0 GPa, 64.0 GPa and 79.6 GPa [24]. It is also interesting that while all the moduli increase with increasing strain, the shear modulus C_{44} increases only slightly. Furthermore, all the moduli, except C_{44}, have nearly the same slope (corresponding to the linear term). These features can be observed clearly from the third-order polynomials given below, which can be conveniently applied in the future to find the strained silicon moduli at a given strain level (corresponding to the lattice difference between silicon and its substrate):

$$B = 101.5 + 312.2\left(\frac{\delta V}{V_0}\right) + 218.6\left(\frac{\delta V}{V_0}\right)^2 + 856.5\left(\frac{\delta V}{V_0}\right)^3 \tag{17}$$

$$C_{11} = 151.6 + 303.1\left(\frac{\delta V}{V_0}\right) + 204.1\left(\frac{\delta V}{V_0}\right)^2 + 845.3\left(\frac{\delta V}{V_0}\right)^3 \tag{18}$$

$$C_{12} = 76.5 + 316.7\left(\frac{\delta V}{V_0}\right) + 225.8\left(\frac{\delta V}{V_0}\right)^2 + 862.1\left(\frac{\delta V}{V_0}\right)^3 \tag{19}$$

$$C_{44} = 84.8 + 97.9\left(\frac{\delta V}{V_0}\right) + 102.6\left(\frac{\delta V}{V_0}\right)^2 + 341.2\left(\frac{\delta V}{V_0}\right)^3. \tag{20}$$

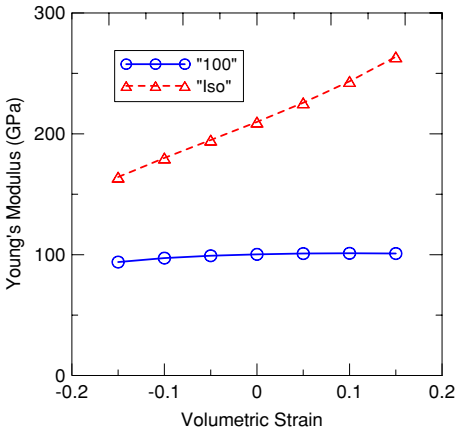

Figure 6. Young's modulus in isotropic silicon and in the (1 0 0)-direction of cubic silicon as functions of the applied volumetric strain in strained silicon.

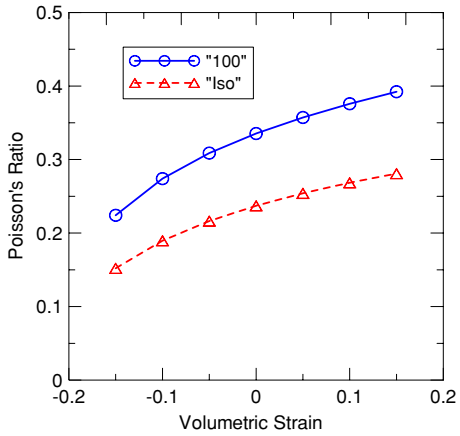

Figure 7. Poisson's ratio in isotropic silicon and in the (1 0 0)-direction of cubic silicon as functions of the applied volumetric strain in strained silicon.

4.3. Effective Young's modulus and Poisson's ratio

Once we obtain the stiffness coefficients as functions of the applied strain, variation of the effective Young's modulus E and Poisson's ratio ν can be also determined. These two parameters are particularly useful in continuum calculations of the mechanical fields within the strained semiconductors under the isotropic approximation. However, as silicon is a cubic material, the elastic properties E and ν will be different in different directions. As an example, we present only E and ν along the (1 0 0)-direction of the crystal. The results of E and ν under the isotropic assumption (C_{11}–C_{12}–$2C_{44} = 0$) are also calculated for comparison. Actually, for given elastic stiffnesses C_{ij}, the elastic coefficients E and ν can be obtained as (we use superscripts '1 0 0' and 'iso' for those along the (1 0 0)-direction and those corresponding to the isotropic case)

$$\nu^{100} = \frac{C_{12}}{C_{11}+C_{12}}, \qquad E^{100} = \frac{(C_{11}-C_{12})(C_{11}+2C_{12})}{C_{11}+C_{12}}, \tag{21}$$

$$\nu^{\mathrm{iso}} = \frac{C_{12}}{2(C_{12}+C_{44})}, \qquad E^{\mathrm{iso}} = \frac{C_{44}(2C_{44}+3C_{12})}{C_{11}+C_{44}}. \tag{22}$$

Substituting the expressions for C_{ij} (equations (17)–(20)) into (21) and (22), we obtain the variation of the elastic coefficients E and ν as functions of the applied strain. The results are shown in figures 6 and 7.

It is very interesting that E^{100} is nearly constant over the whole range of the volumetric strain whilst E^{iso} increases nearly linearly with increasing volumetric strain (figure 6). Furthermore, we also observe from figure 7 that both Poisson's ratios ν^{100} and ν^{iso} increase with increasing volumetric strain, although Poisson's ratio along the (1 0 0)-direction of the crystal is always larger than the isotropic one (at the given strain level).

5. Discussions and conclusions

A simple MD formulation is derived for the material property prediction of strained cubic semiconductors. It combines the simple MD simulation with the basic continuum mechanics. The MD potential used is the Stillinger and Weber potential. We then applied our formulation to the strained silicon and calculated the effective elastic stiffnesses at different levels of volumetric strain. It is found that while C_{11} and C_{12} increase significantly with increasing strain, the shear modulus C_{44} is approximately constant. The MD-simulated values of the stiffnesses at zero volumetric strain agree with those measured experimentally. On the basis of the C_{ij} values, we have also calculated the effective Young's modulus and Poisson's ratio. While Young's modulus along the 1 0 0-direction is almost constant, the 'isotropic' Young's modulus increases with increasing volumetric strain. As for the two Poisson ratios (the 'isotropic' one and the one along the 1 0 0-direction), their values increase with increasing volumetric strain, although Poisson's ratio along the (1 0 0)-direction is always larger than the isotropic one.

We further remark that our results are based on the assumption that silicon is under hydrostatic strain (volumetric strain), with its magnitude being as large as 15%. While this magnitude is moderate for other cubic semiconductors such as InAs/GaAs (i.e., [15]), it could be slightly high for $Si/Si_{1-x}Ge_x$. However, the volumetric strain is strongly dependent on the fraction ratio between Si and Ge. For instance, while $x = 0.1$ in $Si/Si_{1-x}Ge_x$ would result in a small volumetric strain of 2.28%, $x = 0.3$ could give a volumetric strain as high as 7.2% (i.e., [25]). We also point out that the simple assumption of volumetric strain is closely associated with the quantum wire and quantum dot growth modes in cubic semiconductors (i.e., [1]). Other complicated cases, such as layer-by-layer growth, where the two in-plane strains are the same whilst the out-of-plane strain is different, can also be simulated. In that case, one would need to assume different MD initial conditions to the model system.

Acknowledgments

The authors would like to thank the reviewers for their constructive comments which were very helpful in revising the manuscript. The second author (EP) was partially supported

by the Tan Chin Tuan Exchange Fellowship, Nanyang Technology University, Singapore. The first three authors (RZ, EP and PWC) would also like to acknowledge the support from ARO.

References

[1] Bimberg D, Grundmann M and Ledentsov N N 1998 *Quantum Dot Heterostructures* (Chichester: Wiley)
[2] Gleize J, Demangeot F, Frandon J, Renucci M A, Widmann F and Daudin B 1999 *Appl. Phys. Lett.* **74** 703
[3] Jain S C, Willander M, Narayan J and Van Overstraeten R 2000 *J. Appl. Phys.* **87** 965
[4] Jogai B 1998 *Phys. Rev.* B **57** 2382
[5] Park S-H and Chuang S-L 1999 *Phys. Rev.* B **59** 4725
[6] Ghani T *et al* 2003 *Proc. IEDM* p 978
[7] Mcskimin H J and Andreatch P 1964 *J. Appl. Phys.* **35** 2161
[8] Karki B B, Ackland G J and Crain J 1997 *J. Phys.: Condens. Matter* **9** 8579
[9] Stillinger F H and Weber T A 1985 *Phys. Rev.* B **31** 5262
[10] Kluge M D, Ray J R and Rahman A 1986 *J. Chem. Phys.* **85** 4028
[11] Humbird D and Graves D B 2004 *Plasma Sources Sci. Technol.* **13** 548
[12] Menon M, Srivastava D, Ponomareva I and Chernozatonskii L A 2004 *Phys. Rev.* B **70** 125313
[13] Mehl M J, Osburn J E, Papaconstantopoulos D A and Klein B M 1990 *Phys. Rev.* B **41** 10311
[14] Mehl M J 1993 *Phys. Rev.* B **47** 2493
[15] Ellaway S W and Faux D A 2002 *J. Appl. Phys.* **92** 3027
[16] Ray J R 1988 *Phys. Rep.* **8** 109
[17] Birch F 1978 *J. Geophys. Res.* **83** 1257
[18] Tersoff J 1988 *Phys. Rev.* B **38** 9902
[19] Baskes M I, Nelson J S and Wright F A 1989 *Phys. Rev.* B **40** 6085
[20] Biswas R and Hamann D R 1985 *Phys. Rev. Lett.* **55** 2001
[21] Cowley E R 1998 *Phys. Rev. Lett.* **60** 2379
[22] Cook S J and Clancy P 1993 *Phys. Rev.* B **47** 7686
[23] Balamane H, Halicioglu T and Tiller W A 1992 *Phys. Rev.* B **46** 2250
[24] Levinshtein M, Rumyantsev S and Shur M 1996 *Handbook Series on Semiconductor Parameters* vol 1 (Singapore: World Scientific)
[25] Crosby T R, Jones K S, Law M E, Saavedra A F, Hansen J L, Larsen A N and Liu J 2004 *Mater. Res. Soc. Symp. Proc.* **810** C4.12.1